A Calorimetric Study of the Thermal Stability of Barstar and Its Interaction with Barnase†

José C. Martínez,‡ Vladimir V. Filimonov,*,‡,§ Pedro L. Mateo,*,‡ Gideon Schreiber,|| and Alan R. Fersht||

Department of Physical Chemistry, Faculty of Sciences, and Institute of Biotechnology, University of Granada, 18071 Granada, Spain, University Chemical Laboratory, University of Cambridge, Cambridge CB2 1EW, U.K., and Institute of Protein Research, Russian Academy of Sciences, Pushchino, Moscow Region 142292, Russia

Received October 27, 1994; Revised Manuscript Received December 28, 1994®

ABSTRACT: The temperature-induced unfolding of single, double, and triple mutants of barstar, the specific intracellular protein inhibitor of barnase from *Bacillus amyloliquefaciens*, has been studied by high-sensitivity differential scanning calorimetry. The thermal unfolding of barstar mutants, where at least one of the two cysteine residues in the molecule had been replaced by alanine, follows a two-state mechanism at neutral and alkaline pH. The unfolding enthalpy and heat capacity changes are slightly lower than those accepted for highly compact, small, globular proteins. We have found that at pH 2.5, where barstar seems to be in a molten globule state, the protein has a heat capacity between that of the native and the unfolded states and shows some tendency for association. Scanning calorimetry experiments were also extended to the barstar−barnase complex in the neutral and alkaline pH range. The binding constants obtained from DSC studies are similar to those already obtained from other (kinetic) studies. The interaction of barstar and barnase was also investigated by isothermal calorimetry in various buffers within the pH range 6.0−10.0 and a temperature range of 15−35 °C. The favorable enthalpy contribution to the binding is about 4 times higher than the entropic one at 25 °C. The overall data analysis of the combined calorimetric results has led to the thermodynamic characterization of barstar unfolding and the interaction of barstar and barnase over a wide range of temperatures.

The study of biopolymer interaction and recognition is of importance because of the role these interactions play in many crucial biological processes. Thus, the way proteins recognize each other and bind is critical to the understanding of such processes as antigen−antibody interactions, the inhibition of some enzymes, membrane−receptor interactions, and monomer−monomer interactions to give the functional oligomeric protein and can be of invaluable help in protein folding studies (Janin & Chothia, 1990). In addition to structural aspects, the energetic and dynamic characterization of protein recognition is also essential for a rationalization of these macromolecular binding processes. The thermodynamic description of the interaction is best achieved by differential scanning (DSC)[1] and isothermal titration (ITC) calorimetry as direct methods to measure the energetics of these processes and particularly by the complementary combination of both techniques (Martínez et al., 1994).

Here, we show the application of DSC and ITC to study barstar and its interaction with barnase. Both proteins, barnase, an extracellular ribonuclease of 110 residues, and barstar, a specific intracellular barnase inhibitor of 89 residues, are produced by *Bacillus amyloliquefaciens*. Barnase is a very well characterized protein, the structure of which is known both in the crystal state (Maugen et al., 1982) and in solution (Bycroft et al., 1991), which undergoes a reversible, two-state unfolding (Hartley, 1968; Kellis et al., 1989; Martínez et al., 1994). The structure of free barstar has been studied in solution by NMR (Lubienski et al., 1993, 1994), and some of its unfolding properties have also been described (Hartley, 1989; Schreiber & Fersht, 1993b; Khurana & Udgaonkar, 1994). The two proteins form a tight 1:1 complex in solution (Hartley, 1993; Schreiber & Fersht, 1993a), the structure of which has been elucidated (Jones et al., 1993; Guillet et al., 1993; Buckle et al., 1994).

In this paper, we describe a DSC thermodynamic study of the thermal stability of free barstar and that of the barstar−barnase complex in the pH range 6.0−11.0. Wild-type barstar gives rise to complex, sometimes irreproducible, endotherms because of complications caused by the oxidation of the two cysteines, 40 and 82, present in the molecule (Hartley, 1989; Schreiber & Fersht, 1993b). Therefore, single, double, and triple barstar mutants, where at least one of the cysteines was replaced by alanine, were used throughout this work. In addition, the binding of the two proteins has been investigated by ITC in the pH range 6.0−10.0, with different buffer systems of different heats of protonation, and at four temperatures within the range 15−35 °C. The overall data analysis of the two sets of experimental calorimetric results has led to a complete thermodynamic characterization of barstar thermal denaturation and of the barstar−barnase interaction. The results are discussed in the light of the structural information available for the two proteins.

† This research has been supported by BRIDGE Grant BIOT-CT91-0270 from the European Union. P.L.M. also acknowledges financial support from DGICYT Grant PB90-0876 (Spain). J.C.M. is a predoctoral fellow of the DGICYT.

* To whom correspondence should be addressed [telephone, +34-(9)58-243333/1; Fax, +34-(9)58-274258].

‡ University of Granada.

§ Russian Academy of Sciences.

|| University of Cambridge.

® Abstract published in *Advance ACS Abstracts,* April 1, 1995.

[1] Abbreviations: DSC, differential scanning calorimetry; ITC, isothermal titration calorimetry.

0006-2960/95/0434-5224$09.00/0

MATERIALS AND METHODS

Wild-type barnase was purified as described (Serrano et al., 1990). Barstar, its single mutants C40A and C82A (with cysteines 40 or 82 replaced by alanine), double mutant C40A-C82A (DM), and triple mutants C40A-C82A-P48A (TMPA) and C40A-C82A-P48L (TMPL) (with proline 48 of the DM replaced by alanine or leucine, correspondingly) were obtained according to Schreiber and Fersht (1993a). Before the calorimetric experiments, the protein samples were extensively dialyzed against the appropriate buffer. The 1:1 complex of barnase with barstar mutants was usually made before dialysis and passed through a gel-filtration column to remove any traces of monomers. Gel chromatography was performed using a Sephadex G-50 column (1 × 30 cm) at a flow rate of 0.8 mL/min under the appropriate solvent conditions. All chemicals were of analytical grade (Sigma), and distilled, deionized water was used throughout.

The purified protein samples were prepared in Cambridge and sent to Granada where they were stored frozen in 50 mM Tris-HCl buffer, pH 8.0. Before calorimetric experiments, their purity was checked by electrophoresis, both in $NaDodSO_4$ at pH 8.8 and under native conditions with Tris–glycine buffer systems, pH 8.3. According to $NaDodSO_4$ gel electrophoresis, more than 95% of each barstar sample appeared in a major band corresponding to a polypeptide with a molecular mass of about 10 kDa.

The concentrations of the individual proteins were measured spectrophotometrically using the following extinction coefficients at 280 nm (in mg^{-1} mL cm^{-1})—2.21, barnase; 2.22, barstar; 2.26, C40A; 2.16, C82A; 2.21, DM; 2.45, TMPA; and 2.30, TMPL—as determined by the method of Gill and von Hippel (1989). An extinction coefficient of 2.2 mg^{-1} mL cm^{-1} for the barnase–DM complex was also found (other complexes between barnase and barstar mutants were not studied in this work). In all calculations, the molecular masses of barnase and barstar mutants were rounded to 12.4 and 10.2 kDa, respectively.

The calorimetric experiments on barstar and barstar–barnase complexes were routinely performed at a 0.05 M concentration of various buffers: CAPS and glycine were used in the alkaline range; PIPES, HEPES, and sodium citrate at neutral pH; and acetate and glycine at acidic pH. Scanning calorimetry was done in a computerized version of the DASM-4 calorimeter (Privalov & Potekhin, 1986) at heating rates of 0.5, 1, and 2 K/min with sample concentrations of 1.5–4 mg/mL for barstar or barnase alone and 0.6–1.2 mg/mL for the barstar–barnase complex. The reversibility of protein unfolding inside the calorimeter cell and the baseline of the instrument were routinely checked after each protein heating, as described (Privalov & Potekhin, 1986). To calculate the molar partial heat capacity of the protein, from calorimetric records, a partial specific volume of 0.73 mL/g (an average value for small globular proteins) was adopted for barnase, barstar, and their complex. The maximum possible deflection of the real partial specific volumes from the average one (4%) is much lower than the errors in C_p calculations caused by calorimetric baseline shifts from the mean position. The isothermal calorimetry experiments of barnase–barstar complexing were conducted using an isothermal titration calorimeter built at the University of Granada as described by Martínez et al. (1994).

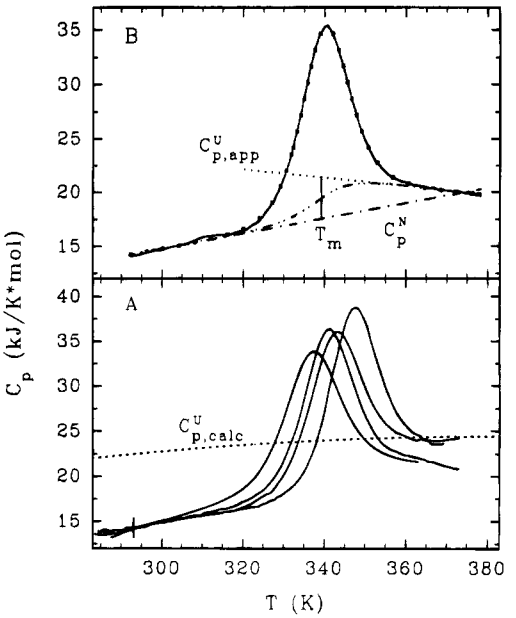

FIGURE 1: (A) Selected temperature dependencies of the partial molar heat capacities of some barstar mutants at various conditions. In order of decreasing stability: DM, 50 mM sodium citrate, pH 6.0, 1.75 mg/mL, 1 K/min; TMPL, 50 mM CAPS, pH 10.0, 1.0 mg/mL, 2 K/min; DM, 50 mM glycine, pH 10.3, 3.2 mg/mL, 1 K/min; DM, 50 mM CAPS, pH 10.8, 2.0 mg/mL, 2 K/min. The DSC traces were aligned to make their C_p coincide at 293 K with an average value of 14.3 kJ/(K·mol) [the vertical bar shows the limits of C_p(293 K) scatter]. The short-dashed line corresponds to the calculated $C^U_{p,calc}(T)$ function (see text). (B) The best fitting of one of the DSC curves for the barstar DM at pH 10.3, 50 mM CAPS, 1 K/min, 2.0 mg/mL. The solid line corresponds to the experimental $C_p(T)$ curve, and dots refer to its best fitting to the two-state model. Curves: best fit of the $C^U_{p,app}(T)$ (•••), $C^N_p(T)$ (– • –), and $C^{int}_p(T)$ (– • • –) functions. The bar at T_m shows the best-fit value of $\Delta C^U_{p,m}$ (eq 4), which in this particular case was 3.9 kJ/(K·mol).

RESULTS

Thermal Stability of Barstar Mutants. Wild-type barstar exhibits a complex unfolding transition upon heating. This problem was attributed (Hartley, 1989) to two cysteine residues (40 and 82) which, as was found later (Guillet et al., 1993; Lubienski et al., 1994), are situated in rather close proximity in the native protein structure. The melting curves of wild-type barstar, determined by DSC in this study, are also rather complex and irreproducible. To avoid all these problems in our DSC studies, we used barstar mutants in which at least one of the cysteines was replaced by alanine. All the barstar mutants exhibit quite simple and reproducible melting curves at neutral and alkaline pH values (Figure 1A). Thus, it seems that the complex unfolding pattern of the wild-type protein does result from the intramolecular cross-bridge formation upon protein heating.

Barstar loses its native conformation in the acid pH range at room temperature (Schreiber & Fersht, 1993b; Khurana & Udgaonkar, 1994) (cf. below) so that its heat-induced unfolding can be studied at only neutral or alkaline pH. These solvent conditions have been used throughout this work to change the stability of the native conformation.

At pH ≥ 6, the reversibility of unfolding for all the barstar mutants studied is rather high (up to 80%), unless the sample had been heated for too long after completion of unfolding. Although there is no dependence of the peak shape and

position on the heating rate, continued heating at high temperatures usually results in a gradual decrease of the area of the main peak. This decrease in the reversibility of the thermal unfolding must result from some irreversible processes that follow the unfolding. Such processes might be, for example, related to irreversible oligomerization of the unfolded polypeptide and/or its chemical modification (Klibanov & Ahern, 1987). No visible precipitates were formed, however, upon heating barstar solutions to 100 °C. In addition, $NaDodSO_4$ gel electrophoresis of all these samples heated inside the calorimeter revealed no additional bands with any molecular mass other than that of intact barstar, which excludes the possibility of chemical degradation of the protein. Conversely, electrophoresis under nondenaturing conditions (pH 8.3) of protein samples heated at pH $\geq$ 6 reveals minor bands with a mobility exceeding that of the native protein (results not shown). This observation suggests chemical modifications and/or incorrect refolding of the barstar mutants after their exposure to high temperatures. The slow kinetics of the irreversible processes following protein unfolding is consistent with chemical modifications. This conclusion has some support from our being unable to refold the protein that had been heated in the calorimeter, even by the addition and slow removal of 6 M urea (the degree of refolding after such treatment was always found by DSC to be incomplete).

The heat capacity of the initial, native state of fresh preparations of barstar mutants, $C_p^N(T)$, linearly increases with temperature in a typical manner for small globular proteins. The following empirical formula was deduced after averaging the initial parts of all the melting curves of barstar mutants:

$$C_p^N(T) = (14.3 \pm 1.5) + (0.08 \pm 0.008)(T - 293.2) \quad [\text{kJ/(K·mol)}] \quad (1)$$

In general, the baseline of the DASM-4 calorimeter has a very reproducible shape, but it can be shifted from its average position, which adds the greatest contribution (about 5−10%, depending on protein concentration) to the overall error in the C_p determination. The dispersion of the initial C_p slopes is usually much smaller as long as the protein solution is well equilibrated against the solvent by dialysis. In our experiments, because of using relatively low concentrations for a small protein, the dispersion of the initial slope also reached 10%. Such changes in the initial slope lead to quite large displacements of the melting curve at high temperature, which complicates the determination of the heat capacity for the unfolded state, $C_p^U(T)$. In fact, the absolute $C_p^U(T)$ values of barstar are much more widely scattered than the $C_p^N(T)$ values, and we also observed a systematic tendency for the apparent heat capacity of the denatured state to decrease with temperature (Figure 1A), instead of remaining almost constant as has been reported for many other small globular proteins (Privalov, 1979, 1989; Privalov et al., 1989; Martinez et al., 1994). Our experience in heat-induced protein denaturation has shown us that many irreversible modifications of the polypeptide chain, similar to those mentioned above, can be accompanied by an exothermic heat effect, which, depending on the kinetics of those processes, might result in an apparent stepwise decrease in the heat capacity, as will be commented upon in the Discussion. Similar decreases in the posttransitional C_p function have also been reported for some other globular proteins (Takahashi & Sturtevant, 1981; Azuaga et al., 1992). Takahashi and Sturtevant (1981) suggested a general procedure of data analysis for such cases, based on a linear approximation of the initial and final heat capacity over the transition temperature range. We have used a similar approach here with minor modifications.

Let us assume that the heat capacities of the initial and final conformational states can be represented as

$$C_p^N(T) = a_n + b_n(T - T_m) \quad (2)$$

$$C_{p,app}^U(T) = a_u + b_u(T - T_m) \quad (3)$$

Here a_n, a_u, b_n, and b_u are independent variable parameters, specific for each individual melting curve. The transition midpoint, T_m, was chosen as a reference temperature for convenience, since this parameter enters into all formulas determining the peak shape and position. If the heat capacities of the initial and final conformations are defined, and we assume that only these two conformations are populated at equilibrium and choose the initial (native) state as the reference one, then any individual function $C_p(T)$ might be described by the equations:

$$\Delta C_{p,app}^U(T) = (a_u - a_n) + (b_u - b_n)(T - T_m) = \Delta C_{p,m}^U + \Delta b_u(T - T_m) \quad (4)$$

$$\delta C_p^{exc}(T) = (\langle \Delta H^U(T) \rangle^2 / RT^2)(K/(1 + K)^2) \quad (5)$$

$$C_p^{int}(T) = C_p^N(T) + \Delta C_{p,app}^U(T)K/(1 + K) \quad (6)$$

$$C_p(T) = C_p^{int}(T) + \delta C_p^{exc}(T) \quad (7)$$

$$\Delta H^U(T) = \Delta H_m^U + \Delta C_{p,m}^U(T - T_m) + \Delta b_u(T - T_m)^2/2 \quad (8)$$

$$\Delta S^U(T) = \Delta H_m^U/T_m + (\Delta C_{p,m}^U - \Delta b_u T_m) \ln(T/T_m) + \Delta b_u(T - T_m) \quad (9)$$

$$K(T) = \exp[(\Delta S^U(T) - \Delta H^U(T)/T)/R] \quad (10)$$

where K is the equilibrium constant of unfolding, $\Delta H^U(T)$ and $\Delta S^U(T)$ are the enthalpy and entropy changes, and $\Delta C_{p,m}^U$ and ΔH_m^U are the variations in the heat capacity and the enthalpy at the transition midpoint, T_m [$K(T_m) = 1$]. These equations contain six independent parameters (a_n, b_n, a_u, b_u, ΔH_m^U, and T_m) to be adjusted by a fitting procedure. Nevertheless, because of the relatively high stability of barstar the unperturbed initial heat capacity, $C_p^N(T)$, was usually measured over a wide temperature range and could be approximated separately with high accuracy, which reduces the number of truly independent adjustable parameters to four.

The application of this fitting procedure to a typical individual melting curve is shown in Figure 1B. Both the linear approximations of the initial and final heat capacities are illustrated, as found by the curve fitting, as well as the $C_p^{int}(T)$, the T_m and the $\Delta C_{p,m}^U$, which in this case comprises as much as 20% of the total peak height. The experimental

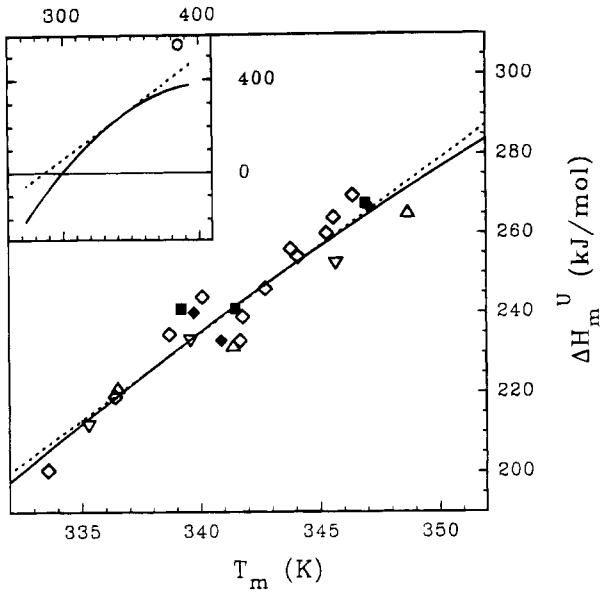

FIGURE 2: Correlation between the unfolding enthalpy and the melting temperature for barstar mutants as found by DSC data analysis: C40A (△), C82A (▽), DM (◇), TMPA (◆), and TMPL (■). Data were obtained in the pH range 6.0−10.8 for DM and 7.0−10.3 for the other mutants. The linear regression through the experimental points (- - -) and the parabolic regression made are as described in the text (—). The insert in the upper left corner shows the same two regressions at wider scales, where the open circle refers to Privalov's "limiting enthalpy" (see text).

melting curve fits the two-state curve very well, as shown by the dotted line in Figure 1B.

The ΔH_m^U values found by applying this fitting procedure to the individual melting curves of various barstar mutants are plotted in Figure 2 *versus* the corresponding melting temperatures. The linear least-squares regression line through these experimental points is represented by the equation:

$$\Delta H_m^U(T_m) = -56 + 4.35(T_m - 273.2) \quad \text{(kJ/mol)} \quad (11)$$

with standard errors in ΔH_m^U and T_m of about ±15 kJ/mol and ±0.5 K, respectively. The average of the $\Delta C_{p,m}^U$ values found by the fitting procedure over the barstar melting range, 334−349 K, was found to be 4.1 kJ/(K·mol) with a standard error as high as ±2.5 kJ/(K·mol).

Barstar Melting at Acid pH. The mutant DM at pH 2.5 does not show a DSC transition similar to that at pH ≥ 6, and neither is its $C_p(T)$ function typical for a completely unfolded protein (Figure 3). At low temperature, the protein has a much higher apparent molar heat capacity than the average value of 14.3 kJ/(K·mol) found for the native protein at 293 K and, at the same time, somewhat lower than the $C_p^U(T)$ value calculated as described in the Discussion (Figure 3). The first heating of the sample in the calorimeter cell resulted in a typical almost linear increase of C_p at temperatures below 325 K. The position and slope of the heat capacity for this initial state do not depend on the heating rate within the limits of experimental error. Increasing the temperature to above 325 K, however, caused a wide endothermic process, followed at about 365 K by a very sharp exotherm. Such sharp exotherms are typical of protein aggregation, and in fact, the position and shape of this exothermic peak depend on the heating rate in a manner expected for a kinetically controlled process. Reheating the sample showed that at low temperatures its apparent heat

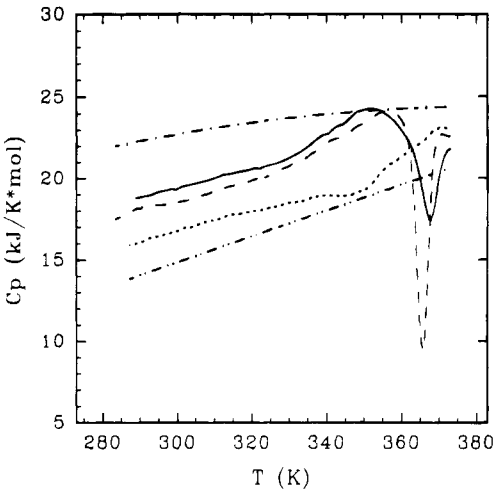

FIGURE 3: Temperature dependence of the partial molar heat capacity of the barstar DM at pH 2.5, 20 mM glycine, 1.9 mg/mL: first heating at 2 K/min (—) and at 1 K/min (− −); second heating at 1 K/min (•••). For purposes of comparison we show the calculated heat capacity of the unfolded state (− • −) and the empirical approximation of the heat capacity of the native state (− •• −).

capacity is much closer to the C_p of the native state than to that of the unfolded one (Figure 3).

The heated protein at pH 2.5 has an increase in light scattering characteristic of an association process. There is an increase in the light scattering of the mutant DM in the order: pH 7.0, pH 2.5 before heating, and pH 2.5 after heating to 100 °C (e.g., the absorbance at 330 nm of these three samples is ≃0, 0.05, and 0.15, respectively, for a concentration of the DM of about 3.5 mg/mL). Size-exclusion chromatography (results not shown) in a Sephadex G-50 column of DM solutions under these conditions showed that the DM at pH 2.5 with or without heating has a very small retention index, very close to the column exclusion volume, whereas the DM at pH 7.0, as well as that at pH 10.0, appears in the DM monomer position. Therefore, the DM clearly behaves as a monomer at pH ≥ 6, while, whatever conformation the protein has at pH 2.5, it shows a certain tendency to association concomitant with an increase in temperature. We also carried out the isothermal calorimetric measurement of the DM denaturation by changing the pH from 7.0 to 2.5 at 25 °C. The expected ΔH value (eq 11) is about 50 kJ/mol, whereas we obtained −95 ± 5 kJ/mol, which means that additional process(es) must occur with a ΔH of approximately 145 kJ/mol. Among other factors (e.g., titration of certain protein groups) this process may well be the association of the protein at pH 2.5, since, for example, the dissociation and unfolding heat of the dimeric CheY molten globule at pH 2.5 has been found to be −155 ± 20 kJ/mol (Filimonov et al., 1993).

DSC of the Barnase−Barstar Complex. Barnase forms a very tight complex with the barstar mutant (DM) at pH 7.0 (almost as tight as with the wild-type barstar) with a dissociation constant of about 2×10^{-13} M (Hartley, 1993; Schreiber & Fersht, 1993a). Such a high affinity should increase considerably, by mass action, the thermal stability of at least one of the components of the complex. This has indeed been observed in DSC experiments (Figure 4), which makes the determination of the binding constant easier.

The barnase−DM complex does not form at pH values below 3.5, and if it does, it is not very soluble in the pH

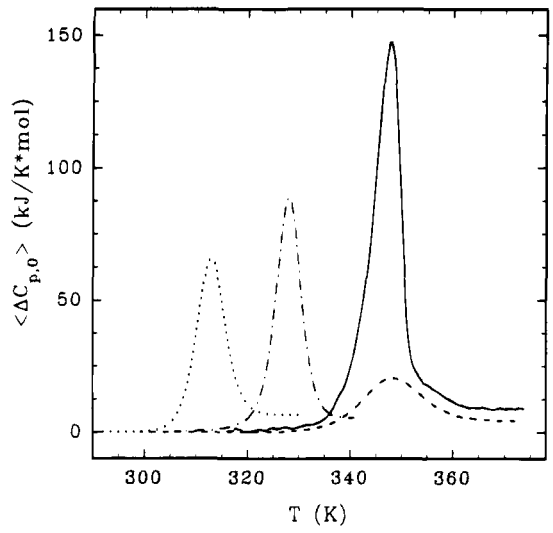

FIGURE 4: Temperature dependence of the $\langle \Delta C_{p,0} \rangle = C_p(T) - C_p^N(T)$ function at pH 7.0, 50 mM PIPES for the DM−barnase complex (—) and of its isolated individual components: DM (− −) and barnase (− • −). The melting of the complex at pH 3.0 is also shown (• • •); it corresponds to that of barnase since barstar is already unfolded and unbound at this pH.

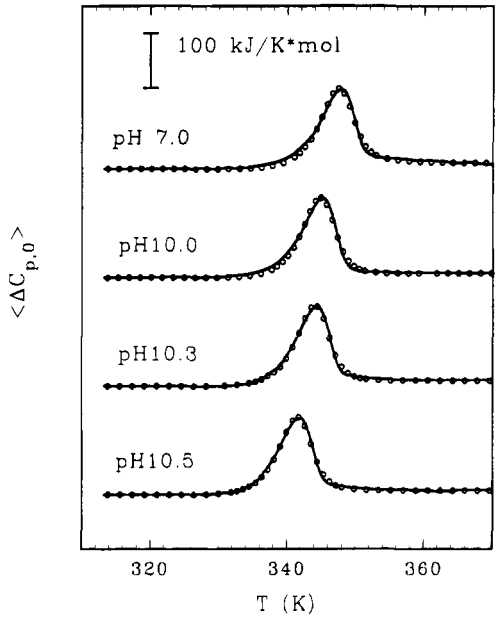

FIGURE 5: Temperature dependence of $\langle \Delta C_{p,0} \rangle$ for the DM−barnase complex at various pH values and their best fittings according to the model of eq 12 in the text. Symbols show the experimental data and solid lines their best fittings.

range 3.5−6.0 (Schreiber & Fersht, 1993a). The inability of barstar to form the complex with barnase at pH ranges around 3 was shown also by the DSC trace, which has only one *symmetric* peak with parameters (T_m and ΔH_m) corresponding to an independent melting of barnase (Figure 4). Hence, at this pH the native conformation of barstar is so energetically unfavorable that, at about 0.1 mM concentration of both proteins in solution, even the high affinity for native barnase cannot compensate for the positive Gibbs energy of barstar folding. Although the solubility of the native complex is high at neutral pH and low temperatures, the unfolding of each component under these conditions is only partially reversible, most probably due to the proximity of their isoelectric points. For example, at pH 6.0 the melting curves of the complex are not reversible on reheating and depend strongly on the heating rate. At pH 7.0 and above the situation alters with a negligible scan-rate effect on the DSC traces and a recovery of the melting profile on sample reheating of at least 60%. It must be emphasized here that the asymmetry observed in the barnase−barstar DSC curves (see Figures 4 and 5) has nothing to do with any irreversible character of the unfolding but is an integral property of any dissociation (or association) process coupled to the unfolding of the protein complex (Brandts & Lin, 1990).

Figure 4 shows that, at pH 7.0, barnase is the component of the complex that becomes more stable (by about 20 K at a working concentration of protein), while under these conditions the complex is only about 2 K more stable than the free DM. Such a low stabilization of barstar means that after dissociation of the complex, accompanied by barnase unfolding, about 40% of barstar molecules can still adopt the native conformation. This native protein fraction should melt in accordance with the unfolding parameters of barstar, i.e., in a rather wide temperature range. Indeed, the unfolding of this barstar fraction was observed as a small shoulder on the right-hand side of the main large peak (Figure 4).

Assuming that under some solvent conditions the temperature-induced unfolding of a 1:1 two-protein complex occurs at equilibrium, one can apply the following reasonable scheme to the DSC data analysis:

$$A^NB^N \overset{K^D}{\rightleftharpoons} A^N + B^N \begin{cases} \overset{K_a^U}{\rightleftharpoons} A^U + B^N \\ \overset{K_b^U}{\rightleftharpoons} A^N + B^U \end{cases} \quad (12)$$

where superscripts N and U refer to the native and unfolded states of the two proteins, A and B, while the equilibrium constants K^D, K_a^U, and K_b^U refer to the dissociation of the complex followed by the independent unfolding of A and B.

The following equations can then be written for this model:

$$f_{ab} + f_{an} + f_{au} = 1 \quad (13)$$

$$f_{ab} + f_{bn} + f_{bu} = 1 \quad (14)$$

$$f_{ab} = [A^NB^N]/P_0 \quad (15)$$

$$f_{an} = [A^N]/P_0 \quad (16)$$

$$f_{au} = [A^U]/P_0 \quad (17)$$

$$f_{bn} = [B^N]/P_0 \quad (18)$$

$$f_{bu} = [B^U]/P_0 \quad (19)$$

$$K^D = [A^N][B^N]/[A^NB^N] = f_{an}f_{bn}P_0/f_{ab} \quad (20)$$

$$K_a^U = f_{au}/f_{an} \quad (21)$$

$$K_b^U = f_{bu}/f_{bn} \quad (22)$$

where the f values are defined in eqs 15−19 and P_0 stands for the molar concentration of the complex in solution. Simple transformations of these formulas lead to a quadratic equation with the following solutions:

$$f_{au} = 2K_a^U/(1 + K_a^U)Z \quad (23)$$

$$f_{bu} = 2K_b^U/(1 + K_b^U)Z \quad (24)$$

$$f_{ab} = 4P_0/QZ^2 \quad (25)$$

where

$$Q = K^D(1 + K_a^U)(1 + K_b^U) \quad (26)$$

$$Z = 1 + (1 + 4P_0/Q)^{1/2} \quad (27)$$

If we define T_d as the temperature at which $Q(T_d) = P_0/2$, then $Z(T_d) = 4$ and $f_{ab} = 0.5$, and T_d can be defined in this manner as the "temperature of complex dissociation" at a given protein concentration. The overall excess enthalpy, $\langle\Delta H_{ab}(T)\rangle$, over the initial state (A^NB^N) is expressed as

$$\langle\Delta H_{ab}(T)\rangle = (1 - f_{ab})\Delta H^D + f_{au}\Delta H_a^U(T) + f_{bu}\Delta H_b^U(T) \quad (28)$$

and the derivative of this function corresponds to the excess heat capacity function, $\langle\Delta C_{p,ab}(T)\rangle$, over the initial state:

$$\langle\Delta C_{p,ab}(T)\rangle = C_p(T) - C_{p,ab}(T) = d\langle\Delta H_{ab}(T)\rangle/dT \quad (29)$$

This function can be found here without difficulty from the experimental DSC data since, given the relatively high stability of the complex, the $C_{p,ab}(T)$ function can easily be approximated by a straight line.

For the purpose of data analysis by curve fitting, the equilibrium constants and other thermodynamic potentials can be expressed by equations similar to eqs 8−10. To reduce further the number of adjustable parameters for curve fitting, we can use here the known temperature dependencies for $\Delta H_a^U(T)$ and $\Delta H_b^U(T)$. That for barnase was obtained in our previous work (Martínez et al., 1994), and to obtain that for barstar we can use eq 11. This leaves us with only three adjustable parameters, ΔH^D, ΔS^D, and ΔC_p^D, defined as

$$\Delta H^D(T) = \Delta H^D(T_{m,b}) + \Delta C_p^D(T - T_{m,b}) \quad (30)$$

$$\Delta S^D(T) = \Delta S^D(T_{m,b}) + \Delta C_p^D \ln(T/T_{m,b}) \quad (31)$$

$$K^D = \exp(-\Delta G^D(T)/RT) = \exp[(\Delta S^D(T) - \Delta H^D(T)/T)/R] \quad (32)$$

where, once more, all the functions are calculated using the complex as the reference state.

In our analysis, the melting temperature of barstar was taken as a convenient reference to reduce extrapolation errors, since barstar alone melts at almost the same temperature as that at which the whole complex breaks down. The results of the fitting of the experimental data for the barstar(DM)−barnase complex, using the general model described above, are shown in Figure 5 and Table 1.

Isothermal Calorimetry of the Barnase−Barstar Binding. We have determined the heat effects of binding between barnase and the barstar DM at various pH values and in different buffers. The latter was necessary since the heats of buffer ionization at neutral and alkaline pH are relatively high, and also the use of various buffers allows one to

Table 1: DSC Values of the Unfolding Enthalpy, ΔH_m^U, and Melting Temperature, T_m, for Isolated Barnase (BN) and Barstar Double Mutant (DM) Samples and Thermodynamic Parameters of the Barnase Interaction with Barstar−DM at 298 K As Found by DSC and ITC

	DSC						ITC[a]			
conditions	T_m(BN) (K)	ΔH_m^U(BN) (kJ/mol)	T_m(DM) (K)	ΔH_m^U(DM) (kJ/mol)	$\Delta H^D(298)$ (kJ/mol)	$\Delta S^D(298)$ [J/(K·mol)]	$K^D(298)$ (10^{-14} M)	$\Delta C_p^D(298)$[b] [kJ/(K·mol)]	$\Delta H^D(298)$ (kJ/mol)	$\Delta n(298)$	$\Delta n(298)$[c]
pH 6.0 (no DSC)									49 ± 2	−0.16 ± 0.06	−0.23 ± 0.06
pH 7.0 (50 mM PIPES for DSC	327.0 ± 0.5	550 ± 20	347.0 ± 0.5	265 ± 15	45 ± 20	−51 ± 5	15 ± 4	0.8 ± 0.1 (62 ± 3)	58 ± 3	−0.37 ± 0.06	−0.31 ± 0.06
pH 10.0 (50 mM CAPS for DSC)	321.6 ± 0.5	510 ± 20	341.6 ± 0.5	245 ± 15	45 ± 20	−93 ± 7	1.2 ± 0.3	0.9 ± 0.1 (71 ± 5)	107 ± 5	0.76 ± 0.06	
pH 10.3 (50 mM CAPS for DSC)	321.4 ± 0.5	507 ± 20	340.0 ± 0.5	240 ± 15	35 ± 20		4.0 ± 1.0	(0.9)			
pH 10.5 (50 mM CAPS for DSC)	320.4 ± 0.5	500 ± 20	338.7 ± 0.5	235 ± 15	54 ± 20		5.5 ± 1.5	(0.9)			

[a] ITC values are corrected for heat buffer effects (Figure 8). The effects of CAPS and PIPES buffers are also shown in parentheses for comparison with the $\Delta H^D(298)$ DSC data. [b] ΔC_p^D values at pH 10.3 and 10.5 were assumed to be the same as that at pH 10.0 and used for extrapolation of the DSC binding parameters to 298 K. [c] The number of protons exchanged on binding, Δn, determined directly by pH-stat.

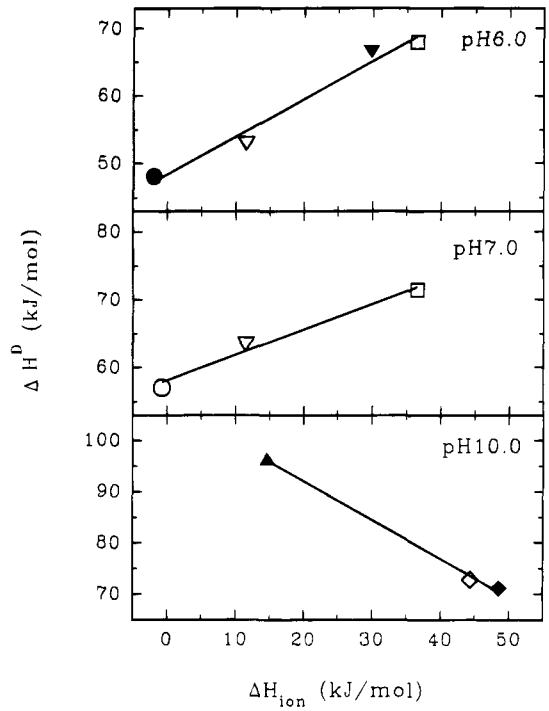

FIGURE 6: Dissociation heats, ΔH^D, of the DM−barnase complex at 25 °C and three pH values plotted *versus* the ionization heat, ΔH_{ion}, of the corresponding buffer: β-glycerophosphate (○); sodium cacodylate (●); PIPES (▽); histidine (▼); imidazole (□); sodium bicarbonate (▲); glycine (◇); CAPS (◆). Solid lines show the linear regressions through the data points.

estimate the proton exchange at binding. We made calorimetric titrations at 15, 20, 25, and 35 °C to obtain the heat capacity increment of binding (experimental points not shown). The heats of the barnase−DM interaction in different buffers at 25 °C are plotted against the heats of ionization of those buffers at three pH values in Figure 6. The straight lines in this figure correspond to the linear regressions through the data points. The slopes of these regression lines should be equal to the number of protons exchanged between the two proteins and the buffer upon binding, whereas their intercepts correspond to the binding enthalpies corrected for the buffer ionization heats. These figures are shown in Table 1 together with other isothermal titration data, as well as the results of the direct determination of the number of exchanged protons using the potentiometric pH-stat technique.

DISCUSSION

In general, heat-induced unfolding of the barstar mutants at the concentrations used in our DSC studies at pH ≥ 6.0 is quite reversible. The DSC peaks are practically independent of scan rate, and the recovery of the melting curves on a second heating of the sample is similar to that of many other globular proteins. Thus, the data analysis in Figure 2 and eq 11 would seem to be correct. Nevertheless, as stated in the results section, reversibility decreases with an increase in both the temperature reached and the time spent at high temperature, as also shown by the CD studies of Khurana and Udgaonkar (1994). Further, there is a systematic tendency for the $C_{p,app}$ to decrease after denaturation (Figure 1A). This behavior usually indicates that the unfolding either deviates from a monomolecular scheme or is highly affected

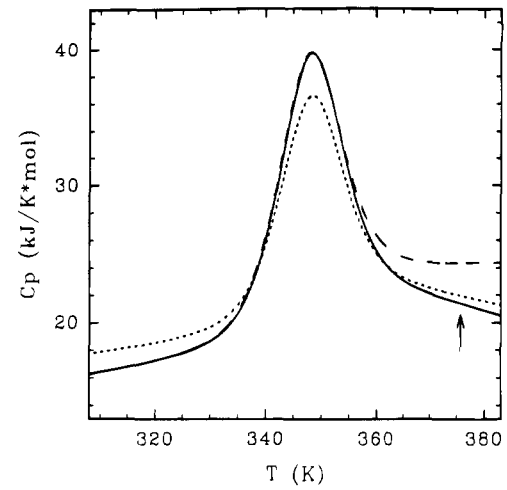

FIGURE 7: Simulations of the DSC curves for the barstar DM using the equilibrium two-state model (− −) and the Lumry−Eyring model with unfolding transition parameters similar to those of the DM at pH 7.0: $C_p^N(T) = 15 + 0.08(T - 293)$; $C_p^U(T) = 24 + 0.01(T - T_m)$; $T_m = 347$ K; $\Delta H_m^U = 265$ kJ/mol. The parameters for the irreversible step (eq 33) were $\Delta H^F = -60$ kJ/mol; $\Delta C_p^F = 0$; $T^* = 435$ K; $E = 90$ kJ/mol; $v = 1$ K/min. First heating (—) and reheating (• • •) were both within the Lumry−Eyring model; the first heating went up to 373 K (shown by the arrow), where the population of the F state reached 20%.

by an irreversible process. The first possibility is not consistent with the results of electrophoresis of samples of barstar. These revealed neither degradation nor aggregation of the polypeptide when it is exposed to high temperatures. Conversely, the lack of any apparent distortion of the $\delta C_p^{exc}(T)$ suggests that the irreversible steps are very slow compared to the folding/unfolding kinetics at temperatures just above the T_m of the protein. If these irreversible steps had significant *exothermic* heat effects, however, even their slow development might distort the $C_p^{int}(T)$ by producing an apparent decrease in the posttransitional heat capacity, as can be demonstrated by the following melting curve simulation (Figure 7) according to the Lumry−Eyring model:

$$N \overset{K^U}{\rightleftharpoons} U \xrightarrow{k^F} F \qquad (33)$$

which has already been successfully used for the analysis of the irreversible DSC melting curves of several proteins (Sánchez-Ruiz et al., 1988; Conejero-Lara et al., 1991). The complete development of this model, assuming there to be no heat effect during the final step, was made by Sánchez-Ruiz (1992) and Lepock et al. (1992). Using their formulas with a reasonable combination of thermodynamic and kinetic parameters, but assuming now that the final step is accompanied by a *negative enthalpy change*, one can simulate melting curves such as that shown in Figure 7. Thus, such a model may explain not only the downward slope of the posttransitional $C_{p,app}$ (Figure 1) but also the properties of the reheating curve, which completely resembles the experimental one. Figure 7 shows why such parameters as ΔH_m^U and T_m are almost unchanged by the existence of the irreversible step, while, conversely, the apparent heat capacity of the unfolded state is completely distorted.

We cannot rule out the possibility that at high temperatures the downward slope of the heat capacity may reflect at least

partially an intrinsic temperature dependence. Therefore, in addition to the linear $C^{U}_{p,app}(T)$ function, we have calculated the heat capacity for the completely unfolded state of barstar according to the method proposed by Makhatadze and Privalov (1990). Within the temperature range used, the $C^{U}_{p,calc}(T)$ function of the DM calculated by this method has a typical parabolic shape (Figure 8), which obeys the following empirical equation, obtained by a least-squares fitting of the calculated points with a second-order polynomial:

$$C^{U}_{p,calc}(T) = 22.0 + 0.043(T - 293.2) - (2.45 \times 10^{-4})(T - 293.2)^2 \quad (34)$$

Subtracting eq 34 from eq 1 gives the following $\Delta C^{U}_{p}(T)$ function:

$$\Delta C^{U}_{p,calc}(T) = 7.5 - 0.037(T - 293.2) - (2.45 \times 10^{-4})(T - 293.2)^2 \quad (35)$$

A comparison of this function with the experimental melting curves (Figure 1A) shows that it is in fact very close to the experimental C_p value in the posttransitional temperature range, although remaining somewhat higher. Nevertheless, the calculated $C^{U}_{p}(T)$ does not show any tendency to decrease in the temperature range 350−380 K, which we observed experimentally at neutral pH. Therefore, to simplify the analysis of the melting curves, we have resorted to a linear $C^{U}_{p,app}(T)$ function instead of a parabolic one.

Another approach to evaluate the unfolding heat capacity increase is to analyze the temperature dependence of the unfolding enthalpy. The quality of the least-squares regression through the experimental data hardly depended upon whether a linear or a quadratic function was used (Figure 2). The simplest approach corresponds to the linear approximation of the $\Delta H^{U}_{m}(T_m)$ (eq 11) with a constant $\Delta C^{U}_{p,m}$ of 4.3 kJ/(K·mol). This value not only compares well with the 4.1 kJ/(K·mol) found for $\Delta C^{U}_{p,m}$ from the average of the curve-fitting results but is also reasonably close to the value of 5.3 kJ/(K·mol) (Figure 8) predicted by eq 35 for an "average" melting temperature of 340 K. It must be emphasized though that the results given here for the DM, as with many other data published for small globular proteins, are of dubious use for any reliable extrapolation of the heat effect to 140 °C or even to 110 °C, for the reasons discussed above. For example, the linear approximation of the specific unfolding enthalpy based on eq 11 passes very close to, although slightly below, the "universal" crossing point of 52 J/g at 110 °C, while the best parabolic approximation of the experimental data, which, according to Privalov et al. (1989), should be more realistic, falls further from that value even at 140 °C (Figure 2).

The question still remains as to what extent the application of the two-state model is valid for barstar unfolding. The applicability of this model can be checked by a comparison of the quality of the fitting with that of any other reasonable model. For instance, the introduction of an additional, intermediate step sometimes improves the quality of curve fitting simply because the fitting procedure acquires more freedom with additional variable parameters. In this case it is necessary not only to compare the quality of the fitting but also to consider the populations of the intermediate state.

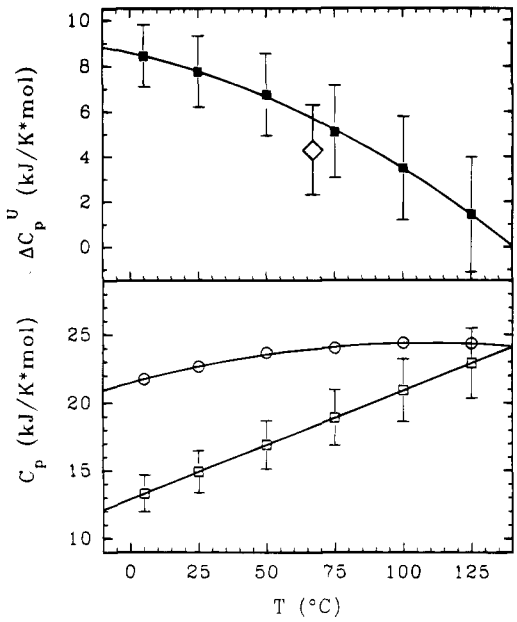

FIGURE 8: Result of the $C^{U}_{p,calc}(T)$ and $\Delta C^{U}_{p,calc}(T)$ calculations of the barstar DM according to Makhatadze and Privalov (1990) (see text). Lower part: calculated $C^{U}_{p,calc}(T)$ values (open circles) and the parabolic least-squares regression through these values; the straight line refers to an empiric $C^{N}_{p}(T)$ linear function found by averaging experimental data (eq 1), where the open squares with bars show the corresponding errors. Upper part: the heat capacity increase upon DM unfolding arising from the difference between the two lines in the lower part, including error bars. The open diamond with error bar corresponds to the average experimental value of $\Delta C^{U}_{p,app}$ at an "average" melting temperature of 340 K (see text).

Thus, when the intermediate state turns out to be only marginally populated, i.e., less than 10% at maximum, it can be concluded that the two-state approach affords a sufficiently good approximation to the experimental data *within the limits of experimental error*. This was actually the case in all our barstar DSC experiments at neutral and alkaline pH.

The DSC traces of barstar at pH 2.5 did not indicate any cooperative unfolding despite the apparent heat capacity of the protein at low temperature being closer to that of the native state than that of the completely unfolded one. Nevertheless, light scattering and chromatography results with this "acid-denatured" form showed that it seems to correspond to protein oligomers rather than to monomers. It appears that protein association can stabilize elements of residual secondary and, to some extent, tertiary structure, in accordance with the molten globule characteristics reported for this "denatured" state (Kurana & Udgaonkar, 1994; Lubienski et al., 1994). Kurana and Udgaonkar (1994) have shown that, although the acidic form of barstar (the A form or molten globule at pH <4) has less secondary and tertiary structure than the native state (pH >5), the former requires higher concentrations of denaturant to unfold than the latter. These authors also describe the unfolding of the A state by urea or GuHCl as a complex, non-two-state transition with at least one intermediate state. All these results are compatible with an association state of barstar at pH 2.5 in our concentration range. It is worth mentioning here that the molten globule state also detected at pH 2.5 for CheY has a strong tendency to form at least dimers in solution (Filimonov et al., 1993). In addition, Sanz et al. (1994) have recently

shown that the A state of barnase undergoes self-association in solution at pH 2.7.

The barnase DSC results shown in Table 1 are new experiments similar to those reported at acid pH (Martinez et al., 1994), with which they correlate very well. The barstar−DM sample mainly used here has been shown to be fully functional both *in vivo* and *in vitro* (Hartley, 1993). The value of ΔG for unfolding, 21.0 ± 1.6 kJ/mol (5.0 ± 0.4 kcal/mol), agrees with that of Schreiber and Fersht (1993b), 4.84 ± 0.18 kcal/mol (both at 25 °C and pH 8.0), obtained from urea denaturation of the DM. The specific enthalpy values of unfolding found for the various mutants used here (Figure 2) are slightly lower at the corresponding T_m than those reported for small, highly compact, globular proteins, whereas the specific ΔC_p of unfolding falls within the lowest limit for these proteins (Privalov, 1979). Barstar has a well-defined hydrophobic core with low solvent accessibility, although the ring of Phe-74 flips freely inside the core, which would indicate that the barstar core is not rigid and well packed but more fluid in character (Lubienski et al., 1994). This character can be reflected in the above-mentioned comparatively low ΔH and ΔC_p values.

DSC and ITC have proved to be very efficient as complementary techniques to characterize the energetics of the barnase−DM interaction. The binding constant at 25 °C, determined from the combined ITC and DSC analysis (Table 1), agrees very well with those calculated from kinetic studies (Hartley, 1989, 1993; Schreiber & Fersht, 1993a), despite the fact that our value had to be extrapolated over a temperature range of 50 °C. The errors in the binding enthalpy obtained by DSC are obviously higher than those directly obtained by ITC because the former were calculated from other, much higher heat effects. Nevertheless, the DSC enthalpy values at 25 °C compare with those obtained from ITC within experimental uncertainty (Table 1). The entropy values shown in Table 1 were obtained from the K_d and ITC enthalpy data, whereas the ΔS values obtained from the DSC data analysis had a higher error (about 30%), just as had the ΔH values.

The barnase−barstar binding is overall both enthalpy- and entropy-driven, although the enthalpy term is about 4 times higher than the entropic one at pH 7.0 at 25 °C. This high negative enthalpy binding value correlates very well with our present knowledge of the structural information of the complex (Hartley, 1993; Jones et al., 1993; Guillet et al., 1993; Buckle et al., 1994). Thus, the barstar−barnase interface is formed by highly polar and charged surfaces, forming a network of polar interactions with 14 hydrogen bonds and several electrostatic bridges, interactions characterized by a few kilocalories per mole [cf. Gillet et al. (1993) and Buckle et al. (1994)]. In addition, a number of well-ordered water molecules are at the interface, some of them forming hydrogen bond bridges between barnase and barstar, allowing for some flexibility at the protein−protein interface. The binding enthalpy should, therefore, come mainly from the creation of this whole net of electrostatic interactions. Given the polar character of the protein binding surfaces and the remaining ordered water, one should expect a comparatively small entropic contribution, as is in fact the case. The negative entropy sign, however, suggests that some water is still released on binding and/or the overall structure becomes less rigid. Apart from the flexible character of the interface region, barstar seems to expand on binding, with localized, minor changes in barnase (Guillet et al., 1993; Buckle et al., 1994). In addition, negative entropy contributions should be expected from strong, localized salt bridges. Nevertheless, a hydrophobic effect should also be taken into account, considering the concomitant negative ΔC_p value of binding, which is generally accepted to have a mainly hydrophobic origin besides the change in internal degrees of freedom. The splitting of the binding ΔC_p, according to the method proposed by Sturtevant (1977), leads in fact to negative values for both the hydrophobic and the vibrational contributions of ΔC_p [−168 and −23 cal/(K·mol), respectively]. Consequently, both a certain release of water molecules and a more flexible protein complex structure are to be expected as a result of barnase−barstar interaction.

NOTE ADDED IN PROOF

During the preparation of this paper another publication on the DSC of the barnase−barstar complex has appeared (Makarov et al., 1994), and a development of the Lumry−Eyring model similar to ours has also been described in detail by Milardi et al. (1994).

ACKNOWLEDGMENT

We thank Dr. A. Parody for allowing us to use the Gill-type ITC and Drs. M. E. Harrous and L. García for helping us in our use of the technique.

REFERENCES

Azuaga, A. I., Galisteo, M. L., Mayorga, O. L., Cortijo, M., & Mateo, P. L. (1992) *FEBS Lett. 309*, 258−260.
Brandts, J. F., & Lin, L.-N. (1990) *Biochemistry 29*, 6927−6940.
Buckle, A. M., Schreiber, G., & Fersht, A. R. (1994) *Biochemistry 33*, 8878−8889.
Bycroft, M., Ludvigsen, S., Fersht, A. R., & Poulsen, F. M. (1991) *Biochemistry 30*, 8697−8701.
Conejero-Lara, F., Sanchez-Ruiz, J. M., Mateo, P. L., Burgos, F. J., Vendrell, J., & Avilés, F. X. (1991) *Eur. J. Biochem. 200*, 663−670.
Filimonov, V. V., Prieto, J., Martínez, J. C., Bruix, M., Mateo, P. L., & Serrano, L. (1993) *Biochemistry 32*, 12906−12921.
Gill, S. C., & von Hippel, P. H. (1989) *Anal. Biochem. 182*, 319−326.
Guillet, V., Lapthorn, A., Hartley, R. W., & Mauguen, Y. (1993) *Curr. Opin. Struct. Biol. 1*, 165−167.
Hartley, R. W. (1968) *Biochemistry 7*, 2401−2408.
Hartley, R. W. (1989) *Trends Biochem. Sci. 14*, 450−454.
Hartley, R. W. (1993) *Biochemistry 32*, 5978−5984.
Janin, J., & Chothia, C. (1990) *J. Biol. Chem. 265*, 16027−16030.
Jones, D. N. M., Bycroft, M., Lubienski, M. J., & Fersht, A. R. (1993) *FEBS Lett. 331*, 165−172.
Kellis, J. T., Jr., Nyberg, K., & Fersht, A. R. (1989) *Biochemistry 28*, 4914−4922.
Khurana, R., & Udgaonkar, J. B. (1994) *Biochemistry 33*, 106−115.
Klibanov, A. M., & Ahern, T. J. (1987) *Protein Engineering* (Oxender, D. L., & Fox, C. F., Eds.) pp 213−218, Alan R. Liss, New York.
Lepock, J. R., Ritchie, K. P., Rodahl, A. M., Heinz, K. A., & Kruuv, J. (1992) *Biochemistry 31*, 12706−12712.
Lubienski, M. J., Bycroft, M., Jones, D. N. M., & Fersht, A. R. (1993) *FEBS Lett. 332*, 81−87.
Lubienski, M. J., Bycroft, M., Freund, S. M. V., & Fersht, A. R. (1994) *Biochemistry 33*, 8866−8877.
Lumry, R., & Eyring, H. (1954) *J. Phys. Chem. 58*, 110−120.
Makarov, A. A., Protasevich, I. I., Lobachev, V. M., Kirpichnikov, M. P., Yakovlev, G. I., Gilli, R. M., Briand, C. M., & Hartley, R. W. (1994) *FEBS Lett. 354*, 251−254.
Makhatadze, G. I., & Privalov, P. L. (1990) *J. Mol. Biol. 213*, 375−384.

Martínez, J. C., El Harrous, M., Filimonov, V. V., Mateo, P. L., & Fersht, A. R. (1994) *Biochemistry 33*, 3919−3926.
Mauguen, Y., Hartley, R. W., Dodson, E. J., Dodson, G. G., Bricogne, G., Chothia, C., & Jack, A. (1982) *Nature 297*, 162−164.
Milardi, D., La Rosa, C., & Grasso, D. (1994) *Biophys. Chem. 52*, 183−189.
Privalov, P. L. (1979) *Adv. Protein Chem. 33*, 167−241.
Privalov, P. L. (1989) *Annu. Rev. Biophys. Biophys. Chem. 18*, 47−69.
Privalov, P. L., & Potekhin, S. V. (1986) *Methods Enzymol. 114*, 4−51.
Privalov, P. L., & Makhatadze, G. I. (1990) *J. Mol. Biol. 213*, 385−391.
Privalov, P. L., Tiktopoulo, E. I., Venyaminov, S. I., Griko, Y. V., Makhatadze, G. I., & Khechinashvili, N. N. (1989) *J. Mol. Biol. 205*, 737−750.
Sanchez-Ruiz, J. M. (1992) *Biophys. J. 61*, 921−935.
Sanchez-Ruiz, J. M., Lopez-Lacomba, J. L., Cortijo, M., & Mateo, P. L. (1988) *Biochemistry 27*, 1648−1652.
Sanz, J. M., Johnson, C. M., & Fersht, A. R. (1994) *Biochemistry 33*, 11189−11199.
Schreiber, G., & Fersht, A. R. (1993a) *Biochemistry 32*, 5145−5150.
Schreiber, G., & Fersht, A. R. (1993b) *Biochemistry 32*, 11195−11203.
Serrano, L., Horovitz, A., Avron, B., Bycrosft, M., & Fersht, A. R. (1990) *Biochemistry 29*, 9343−9352.
Sturtevant, J. M. (1977) *Proc. Natl. Acad. Sci. U.S.A. 74*, 2236−2240.
Takahashi, K., & Sturtevant, J. M. (1981) *Biochemistry 20*, 6185−6190.

BI942516Z